Turkish Journal of Electrical Engineering & Computer Sciences

http://journals.tubitak.gov.tr/elektrik/

Research Article

Turk J Elec Eng & Comp Sci
(2018) 26: 2779 – 2792

doi:10.3906/elk-1804-163

Detecting slow wave sleep and rapid eye movement stage using cortical effective connectivity

Aminollah GOLROU[1], **Ali SHEIKHANI**[1,*], **Ali MOTIE NASRABADI**[2], **Mohammad Reza SAEBIPOUR**[3]

[1]Department of Biomedical Engineering, Science and Research Branch, Islamic Azad University, Tehran, Iran
[2]Department of Biomedical Engineering, Shahed Univrsity, Tehran, Iran
[3]Department of Neuroscience, Birjand University of Medical Sciences, Birjand, Iran

Received: 21.04.2018 • **Accepted/Published Online:** 17.10.2018 • **Final Version:** 29.11.2018

Abstract: In recent neuroimaging research, there has been considerable interest in identifying neuromarkers of sleep. Automatic slow wave sleep (SWS) and rapid eye movement (REM) are two known phases of sleep. However, the level by which those changes contribute to brain interactions has not been well characterized. In recent years, it has been shown that brain connectivity measuring can be helpful in investigation of behavioral states of the brain. By considering the fact that brains have different states in different stages of sleep, the present work employs effective connectivity and machine-learning analysis to quantify and classify SWS and REM stages of sleep. We examine low-density 12-channel EEG data from 8 healthy participants during a full night of sleep. Data were epoched into 30-s windows and SWS and REM stages were labeled by a sleep consultant. Effective connectivity was quantified using a directed metric, generalized partial directed coherence, and measures were used as input features for a machine-learning system. A support vector machine classifier was used to solve 2 binary problems of REM vs. nREM and SWS vs. nSWS. Findings revealed an excellent balanced accuracy of 89.80% in REM detection and 87.32% in SWS detection. Overall, our work demonstrates a successful application of effective connectivity analysis and machine learning for sleep neuromarkers in EEG.

Key words: Sleep staging, effective connectivity, slow wave sleep, rapid eye movement, electroencephalography

1. Introduction

Electroencephalography (EEG) provides a valuable tool for the study of spontaneous brain activity. Scalp potentials measured with EEG allow the classification of sleep into some categorical stages. Human sleep can be divided into rapid eye movement (REM) sleep and nonrapid eye movement (non-REM) sleep. Non-REM sleep can be further classified into Stage 1 (N1), Stage 2 (N2), and slow wave sleep (SWS or N3) according to the American Academy of Sleep Medicine (AASM) rules[1]. Among these sleep stages, SWS has been considered to be the most restorative sleep stage [2]. However, as sleep quality declines with aging, the total amount of SWS decreases drastically [3]. In addition, abnormal SWS has also been found to be correlated with a variety of clinical problems including acute-phase immune system response [4], diabetes risk [5], memory consolidation [6], psychiatric disorders [7], and hypertension [8].

In-depth understanding of these SWS-related problems can be gained by performing long-term sleep architecture monitoring on a large population. Conventionally, sleep stages are scored using the electroencephalo-

*Correspondence: sheikhani_al_81@srbiau.ac.ir

gram (EEG), electromyogram (EMG), and electrooculogram (EOG) signals obtained by a polysomnography (PSG) study. Thus, a large-scale sleep architecture monitoring study would require an intensive amount of work. Manual sleep staging is also tedious, time-consuming, and error-prone. In response to these challenges, many automatic sleep staging methods using statistical learning or artificial intelligence techniques have been developed [9–15].

Sleep staging also can be used as a part of sleep studies. For example, many researchers try to improve some function of sleep such as long-term memory consolidation [16], homeostatic regulation of synaptic connectivity [17], and synaptic potentials triggered by learning [18]. Recent studies try to improve these functionality by stimulating the brain including sleep slow waves induction [19–22], memory consolidation [23–25], and sleep spindles enhancement [26, 27]. In many of these studies it is necessary to detect the SWS or REM sleep stage, which is basis of the presented study.

In some studies, it is shown that brain connectivity changes by changing the state of brain [28–30]. There are three levels of brain connectivity: structural, functional, and effective connectivity. Structural connectivity refers to the pattern of anatomical links in the brain, functional connectivity refers to statistical dependencies of different regions of the brain, and effective connectivity refers to causal interactions between distinct units within a nervous system. The units correspond to individual neurons, neuronal populations, or anatomically segregated brain regions. Thus, tracking brain connectivity may help in designing a sleep staging system and this study is focused on REM and SWS sleep stages. There are some basic methods to estimate brain effective connectivity, such as the Granger causality index (GCI)[31], directed transfer function (DTF)[32], and partial directed coherence (PDC)[33]. GC is a time domain effective connectivity measure that is defined as the logarithm of the ratio of residual variance for one channel to the residual variance of the two-channel model. Information that can be extracted from spectral characteristics of EEG signals, especially in sleep studies such as sleep staging, plays important roles. DTF and PDC are the effective connectivity estimators that are defined in the frequency domain. This study uses generalized partial directed coherence (GPDC) [34], which is a multivariate directed measure that assumes a multivariate autoregressive (MVAR) model for the data and only measures direct connections.

Many other studies tried to detect different sleep stages by using a wide range of features of EEG signals, such as time-domain features, frequency-domain features, and nonlinear features. This study tries to show that there are significant changes in effective connectivities of different areas of the brain by changing sleep states and also it uses effective connectivity values as a feature set to detect some specified sleep states.

2. Materials and methods

2.1. Participants and EEG recordings

For this study, EEG signals are recorded from eight male participants. This recording is a part of a project that tries to investigate the effect of acoustic stimuli in the SWS stage in sleep quality. None of the participants had any medical disorders or neurological disorders, nor were they taking any drugs to sleep. The data are recorded in two nights and only the data from the second night are used. EEG signals are recorded in 12 channels (Fp1, Fp2, Fz, T7, T8, C3, C4, Cz, Pz, FO7, FO8, and Oz) and referenced to an average of electrodes attached to both earlobes or mastoids. Electrode placement was done for each participant 1 h before their usual sleep time. The sampling rate for the EEG recording was 250 Hz and EEG signals were filtered by a high-pass filter of 0.3 Hz and a low-pass filter of 50 Hz. All 30-s epochs of 12-channel EEG signals were sleep scored by an expert according to the AASM criteria.

Table 1 presents EEG recorded information about the number of all epochs for each participant and number of sleep stages epochs for each of them.

Table 1. Information of recorded EEG dataset.

Subject	Number of 30-s epochs	Epochs in each stage				
		Wake	N1	N2	SWS	REM
1	896	95	102	348	242	109
2	889	201	72	333	152	131
3	726	16	81	293	233	103
4	986	105	131	352	249	149
5	847	183	59	253	188	164
6	721	52	87	306	123	153
7	959	84	99	352	257	167
8	818	10	62	314	305	127
Total	6842	787	652	2551	1749	1103

Two approaches are considered to divide the dataset into train and test subsets: subject-based and not subject-based. In the subject-based approach all of the dataset is randomly divided into two subsets of train and test subsets with population of 3421, and in not subject-based approach the data of four subjects are randomly selected for training the classifier and data of the others are selected for testing (this approach is repeated until all possible combinations are achieved). Because of the unequal size of samples in each stage of sleep it is common that the whole sample is randomly divided into train and test subsets without considering the number of samples in each stage [35, 36].

2.2. Effective connectivity estimation

Partial directed coherence (PDC) is a frequency domain description of the directed linear relationship between pairs of time series $x_i(n)$ and $x_j(n)$. GPDC is defined to circumvent the numerical problem associated with time series scaling in PDC. For simultaneous EEG recordings from m channels, $\mathbf{x}(n)$ is represented by a multivariate time series as in Eq. (1).

$$\mathbf{x}(n) = \begin{bmatrix} x_1(n) \\ x_2(n) \\ \vdots \\ x_m(n) \end{bmatrix} \tag{1}$$

Effective connectivity estimators usually use a MVAR to model multivariate time series as in Eq. (2).

$$\mathbf{x}(n) = \sum_{l=1}^{p} \mathbf{A}(l)\mathbf{x}(n-l) + \mathbf{w}(n) \tag{2}$$

Here, p is the model order, $\mathbf{w}(n)$ is a Gaussian stationary innovation process, and $\mathbf{A}(.)$ is an $m \times m$ matrix that includes coefficients of the MVAR model. Matrix $\mathbf{A}$ and $\sigma_{\mathbf{w}}$ (which is the covariance matrix of $\mathbf{w}$) are

used in the GPDC method to estimate effective connectivity in the frequency domain via Eq. (3).

$$\pi_{i,j}(f) = \frac{\frac{1}{\sigma_{ii}}\bar{A}_{ij}(f)}{\sqrt{\sum_{k=1}^{m}\frac{1}{\sigma_{kk}^2}|\bar{A}_{kj}(f)|^2}} \tag{3}$$

Here, σ_{ii} is the ith element in the main diagonal of $\sigma_{\mathbf{w}}$ and $\bar{A}_{ij}(f)$ is the Fourier transform of $\mathbf{A}$'s elements as in Eq. (4).

$$\bar{A}_{ij}(f) = \begin{cases} 1 - \sum_{l=1}^{p} a_{ij}(l)e^{-j2\pi fl}, & \text{where} \quad i = j \\ -\sum_{l=1}^{p} a_{ij}(l)e^{-j2\pi fl}, & \text{otherwise} \end{cases} \tag{4}$$

Here, $j = \sqrt{-1}$, f is frequency, and $a_{ij}(l)$ is element (i,j) of matrix $(A)(l)$. $\pi_{i,j}(f)$ indicates effective connectivity (or Granger causality) from signal $x_j(n)$ to $x_i(n)$ at the frequency of f. To extract connectivity from multichannel EEG signals, the value of some parameters must be initialized, such as model order (p) and length of window. The reliable value of these two parameters is dependent on the significance of the MVAR model. The most common approach for model order selection involves selecting a model order that minimizes the information criteria evaluated over a range of model orders. The Akaike information criterion (AIC) [37] is one of the commonly used information criteria and it is used in this study to select the model order. Local stationarity of the EEG signal and a sufficient amount of data for model fitting must be considered in selecting the length of the window. By using the SIFT toolbox [38], proper values are set as window length of 1 with 0.5 second overlap and model order of 15 is selected.

2.3. Channel selection and classification

After fitting the model, effective connectivity of each 30 s (epoch) of 12-channel EEG signals are extracted using Eq. (3). For each epoch there is a 4-dimensional GPDC connectivity tensor (CT) with size of $m \times m \times n_w \times n_f$, where m is number of channels ($m = 12$), n_w is number of windows ($n_w = 59$), and n_f is number of frequencies that are discretized between 0.3 and 50 Hz ($n_f = 101, f = \{0, 0.5, 1, ..., 50\}$).

Frequency subband power of EEG signals is one of the most important features used in manual sleep staging. This study uses the average of estimated connectivity in the delta (<4 Hz), theta (4–7 Hz), alpha (8–15 Hz), and beta (16–31 Hz) subband frequencies. By this averaging, the CT tensor is divided into four 3-dimensional tensors, CT_{Delta}, CT_{Theta}, CT_{Alpha}, and CT_{Beta}, with size of $m \times m \times n_w$. Also, there are two important concepts of connectivity that are considered in this study: magnitude and variation through time. By averaging and calculating the standard deviation of four presented tensors through time, eight new connectivity matrices (CMs) are extracted for each of the 30-s epochs of EEG signals using Eq. (6).

$$
\begin{aligned}
CT_{subband(i,j,w)} &= \frac{\sum_{f \in subband} \pi_{i,j}^{w}(f)}{n_{f\,subband}} \\
\overline{CM}_{subband(i,j)} &= \frac{\sum_{w=1}^{n_w} CT_{subband(i,j,w)}}{n_w} \\
CM^{\sigma}{}_{subband(i,j)} &= \sqrt{\frac{\sum_{w=1}^{n_w} (CT_{subband(i,j,w)} - \overline{CM}_{subband(i,j)})^2}{n_w}}
\end{aligned}
\tag{5}
$$

Here, $\pi_{i,j}^{w}(f)$ is GPDC connectivity estimation of x_j to x_i in frequency of f for the wth window of the epoch and $n_{f\,subband}$ is number of frequencies in the specified subband. $\overline{CM}_{subband(i,j)}$ and $CM^{\sigma}{}_{subband(i,j)}$ are calculated for all four subbands. For each 30-s epoch there is a feature vector that consists of 1152 features ($m \times m \times number\ of\ subbands \times 2(\overline{CM}$ and $CM^{\sigma})$) and it is necessary to select some best features to feed the classifier. To select the best features, the t-statistic is employed as in Eq. (6).

$$
t_{(d_1,d_2)} = \frac{m_{d_1} - m_{d_2}}{\sqrt{\frac{\sigma_{d_1}^2}{n_{d_1}} + \frac{\sigma_{d_2}^2}{n_{d_2}}}} \tag{6}
$$

Here, m_d, σ_d, and n_d are the average, standard deviation, and population size of the distribution of d, respectively.

The greater value of t presents more separability of a feature. To select the channels that are significantly varied by changing the sleep stages, the t-value is used while considering the P-value. Figure 1 shows estimated connectivity averages of $\overline{CM}$ that are significantly varied in different sleep stages (P-value <0.05) and 20 greater t-values. In this figure and in Figure 2, line color is related to magnitude of connectivity and arrows show the direction.

The feature vector for each 30-s epoch is constructed by 160 connectivity values that consist of 20 greater t-values extracted from $\overline{CM}$ and CM^{σ} in each of four EEG subbands. A support vector machine (SVM) classifier with error-correcting output codes (ECOCs) [39] is used in this study to classify EEG epochs into two binary sets of sleep stages (non-REM vs. REM and non-SWS vs. SWS stage). The results in this study are presented by three measures as sensitivity, accuracy, and Cohen's kappa [40]. The sensitivity of a specific stage measures the proportion of the stage that is correctly identified and accuracy measures the proportion of all stages that are correctly identified. In classification problems, when classes have the same number of samples, accuracy can evaluate the classifier effectively. However, if classes have an unequal number of samples, the accuracy will be biased. Cohen's kappa coefficient (k) is a more robust measure than accuracy and takes into account the possibility of agreement occurring by chance. In a two-class problem, k can be computed as in Eq. (7).

$$
\begin{aligned}
k &= \frac{p_o - p_e}{1 - p_e} \\
p_e &= \frac{1}{N^2} \sum_{m} n_{m,1} n_{m,2}
\end{aligned}
\tag{7}
$$

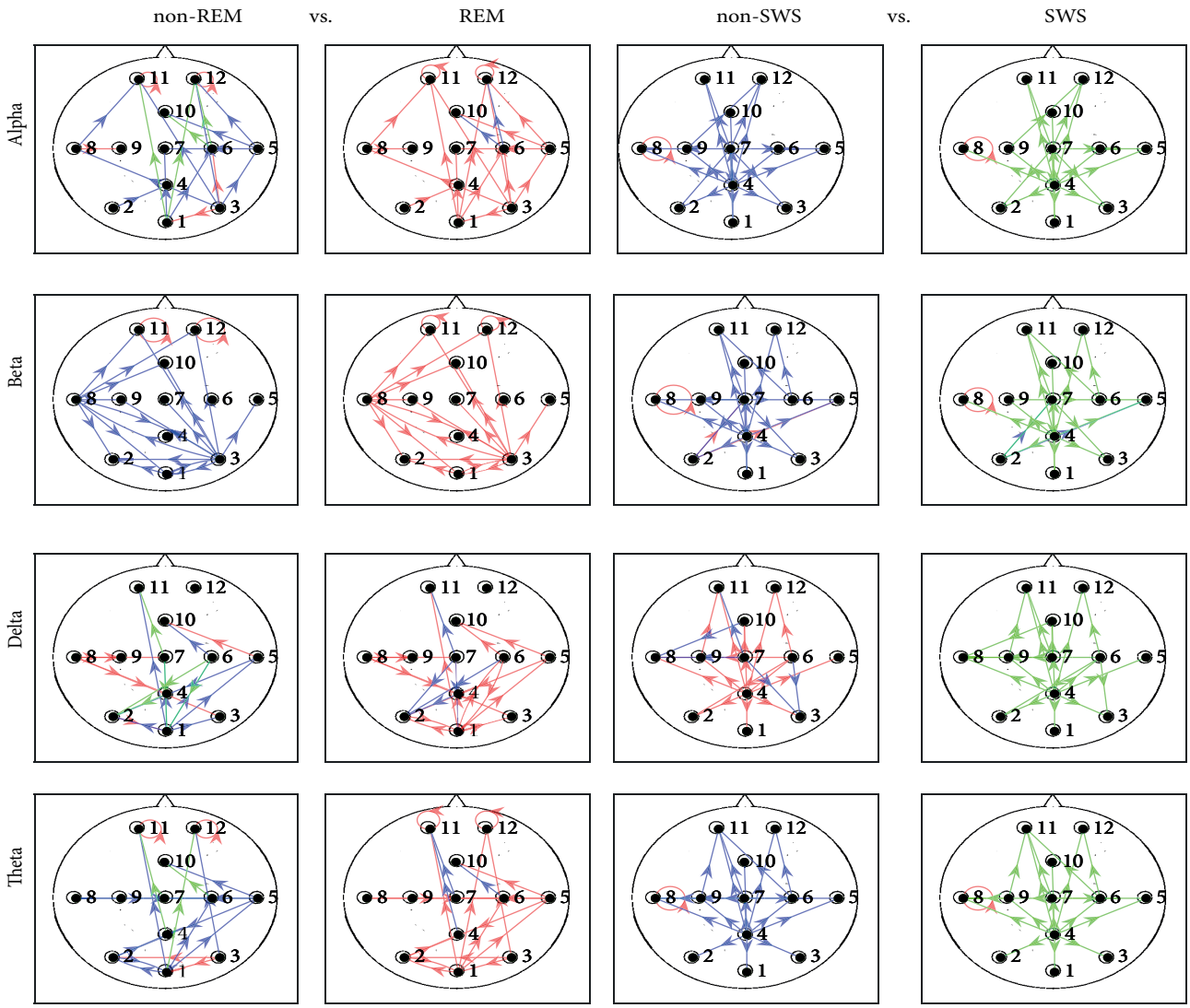

Figure 1. The 20 greater t-value connectivities between channels that are significantly different in two sets of sleep stages. The two left columns present the connectivities between channels whose values are significantly (P-value <0.05) different in non-REM and REM stages and the two right columns present the connectivities between channels whose values are significantly different in non-SWS (N1 and N2 stages) and SWS in four EEG subbands. The color of presented connectivities is related to magnitude of connectivities (red, blue, and green color is high(>0.03), medium (<0.03 and >0.015), and low (<0.015) strength, respectively).

Here, p_o is accuracy and p_e is the hypothetical probability of chance agreement. For class m, $n_{m,i}$ is the number of times rater i predicted m. N is the number of samples.

3. Results and discussion

Figure 1 shows that there are significant changes in magnitude of effective connectivity between some channels and it can be shown that there are also significant changes in variation of connectivities in different sleep stages. Figure 2 presents top 20 t-value standard deviations of channels' effective connectivity. In this figure line color is related to the value of standard deviation of connectivities and just the top 20 significant connectivities are presented.

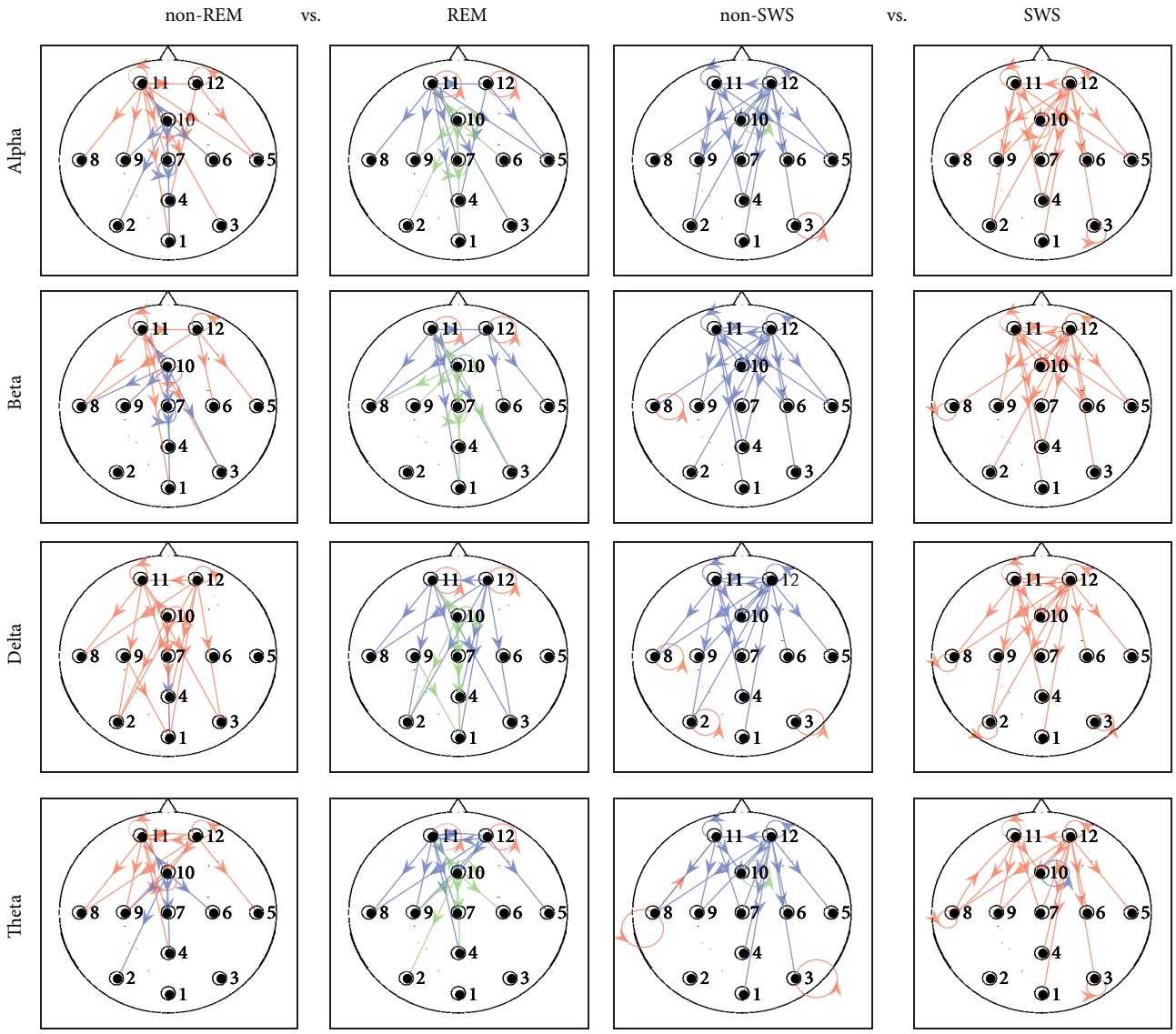

Figure 2. The 20 greater t-value standard deviations of connectivity between channels that are significantly different in two sets of sleep stage. The two left columns present the standard deviation of connectivities between channels whose values are significantly (P-value <0.05) different in non-REM and REM stages and the two right columns present the standard deviation of connectivities between channels whose values are significantly different in non-SWS and SWS in four EEG subbands. The color of presented connectivities is related to the standard deviation of connectivities (red, blue, and green color is high(>0.15), medium (<0.15 and >0.075), and low (<0.075) standard deviation, respectively).

Changes in magnitude of connectivities between channels of EEG signals are notable. In the non-REM stage, magnitudes of connectivities are significantly less than in the REM stage. On the other hand, connectivities in the non-SWS stage have greater magnitude than in the SWS stage (Figure 1). Conversely, connectivities in non-REM and SWS stages have more variation (standard deviation) than REM and non-SWS, respectively (Figure 2). By comparing Figure 1 and Figure 2 it is inferable that in these stages, magnitude and variation of connectivities have an inverse relationship. The connectivities that have greater magnitude in REM and non-SWS stages versus non-REM and SWS have less variation.

As mentioned, the value of connectivities (magnitude and standard deviation) that are used in Figure

1 and 2 ($\overline{CM}$ and CM^{σ}) are considered as the feature vector to train a SVM classifier. The SVM classifiers have some hyperparameters that must be set in the training phase. In this study these hyperparameters are set practically as kernel function of Gaussian, kernel scale of 24, and box constraint of one. Also, all elements of $\overline{CM}$ and CM^{σ} are normalized by standard score method [41] using the average and standard deviation of each element over the training subset.

The built-in SVM classifier of MATLAB 2017 software is used to train SVM classifiers. In each of the following experiments, to find the best value of hyperparameters such as kernel scale and box constraint (C) of a RBF based SVM classifier, 10-fold cross-validation is performed on the training set of data. First, the training set is used to find the best value of hyperparameters by performing a 10-fold cross-validation experiment and then the whole training set is used to train the optimized SVM classifier. Two SVM classifiers are trained to classify the 30-s epochs of EEG signals into non-REM and REM stages and then into non-SWS and SWS stages for both subject-based and not subject-based approaches. Table 2 presents the results of testing the trained and optimized classifier to detect REM stage for the not subject-based approach.

Table 2. Confusion matrix and result of classifying epochs into non-REM and REM stages for not subject-based approach.

		Expert's score	
		Non-REM	REM
Classifier's score	Non-REM	2809	147
	REM	42	423
Sensitivity		98.52%	74.21%
Accuracy		94.48%	
Kappa		0.76	

Table 2 shows the confusion matrix of testing the SVM classifier, sensitivity of REM and non-REM detection, accuracy, and kappa coefficient. It can be seen that, because of the unequal number of samples in each class, the ratio of accuracy and kappa present different values and accuracy is biased to the non-REM stage. The trained SVM classifier achieves accuracy of 94.48% with Cohen's kappa of 0.76.

In Table 3 results of testing the second SVM classifier to classify epochs into SWS and non-SWS stages are presented for the not subject-based approach.

Table 3. Confusion matrix and result of classifying epochs into non-SWS and SWS stages for not subject-based approach.

		Expert's score	
		Non-SWS	SWS
Classifier's score	Non-SWS	1488	116
	SWS	83	789
Sensitivity		94.72%	87.18%
Accuracy		91.96%	
Kappa		0.83	

The second SVM classifier can detect the SWS stage by sensitivity of 87.18%. The accuracy and Cohen's kappa of the classification are 91.96% and 0.83, respectively. In the second case (SWS detection), the kappa

value is closer to the accuracy than in the first case (REM detection) because of less difference between the number of samples in two classes (in the first case, the number of samples in the two classes is 2851 (non-REM) and 570 (REM); in the second case, the number of samples in the two classes is 1571 (non-SWS) and 905(SWS)). Thus, the accuracy is less biased to one class.

Also, in the subject-based approach, two previous experiments are repeated for all possible combinations of selecting subjects for training and testing, and Tables 4 and 5 present the results of REM and SWS detection. In the confusion matrix of these tables the average and standard deviation values for all possible combinations are presented (Average ± standard deviation) and all evaluation metrics are presented according to average confusion matrices.

Table 4. Confusion matrix and result of classifying epochs into non-REM and REM stages for subject-based approach.

		Expert's score	
		Non-REM	REM
Classifier's score	Non-REM	2736.81 ± 53.32	175.81 ± 12.66
	REM	126.23 ± 25.83	389.39 ± 18.25
Sensitivity		95.59%	68.89%
Accuracy		91.19%	
Kappa		0.67	

Table 5. Confusion matrix and result of classifying epochs into non-SWS and SWS stages for subject-based approach.

		Expert's score	
		Non-SWS	SWS
Classifier's score	Non-SWS	1463.55 ± 13.22	176.51 ± 7.81
	SWS	73.68 ± 25.24	732.14 ± 8.63
Sensitivity		95.21%	80.57%
Accuracy		89.74%	
Kappa		0.78	

The lower value of accuracy and Cohen's kappa shows that the estimated effective connectivities using GPDC in different sleep stages are not subject-invariant and connectivities in specific sleep stages vary by changing the subject, especially in the REM stage.

Table 6 presents results of some studies that tried to detect REM or SWS stages. Each of these studies used a variant method to detect SWS or REM, such as time and frequency domain. Not all of these studies used the same measures for evaluation. For those studies for which it was possible, accuracy and Cohen's kappa are calculated and presented.

In the proposed cases (SWS and REM detection), because of the unequal number of samples for classes, Cohen's kappa is an efficient measure to evaluate the efficiency of the method. In the case of SWS detection, the accuracy is less than in some other studies and the value of Cohen's kappa of this study is greater than in other studies.

In the case of REM detection, just as in Imtiaz et al.'s study, kappa and accuracy are presented and the result of the proposed study is better than that study. However, sensitivity (Sen) and selectivity (Sel) (also

Table 6. Performance comparison with other studies.

Study	Method	REM /Non-REM		SWS /Non-SWS	
		Accuracy	Kappa	Accuracy	Kappa
Kubicki et al. [42]	_	_	_	92	0.62
Durka et al. [43]	Adaptive time-frequency approximation	_	_	88	0.72
Virkkala et al. [44]	Cross-correlation of EOG channels and beta power	_	_	93	0.70
Su et al. [45]	The waveform pattern of the EEG	_	_	97.2	0.66
Imtiaz et al. [46]	Spectral edge frequency and power of signals	88.52	0.61	_	_
		80.6(Sen) 74.8(Sel)		_	_
Liang et al. [47]	MSE, AR model	85.4(Sen) 78.8(Sel)		_	_
Ronzhina et al. [48]	Spectral power	82.3(Sen)		_	_
Berthomier et al. [35]	Spectral and temporal features	63.0(Sen) 91.7(Sel)		_	_
This study (not subject-based)	Average and STD of effective connectivities	94.48	0.76	91.96	0.83
		74.21(Sen) 90.97(Sel)			
This study (subject-based)	Average and STD of effective connectivities	91.19	0.97	89.74	0.78
		68.89(Sen) 75.52(Sel)			

known as positive predictive value or PPV) of the proposed study in the case of REM detection are comparable to those of other studies.

Also, to show the potential of the effective connectivity values as a feature set, the same procedure is done to classify EEG epochs into four classes as sleep stage N1, N2, SWS, and REM. The SVM classifier with an ECOC model is used for multiclass classification and the same as previous routine optimum hyperparameters are found by evaluating the classifier using 10-fold cross-validation on the training set. The results of testing the final classifiers in the subject-based and not subject-based approaches are presented in Tables 7 and 8.

Table 7. Confusion matrix and result of classifying epochs into four stages for not subject-based approach.

		Expert's score			
		N1	N2	SWS	REM
Classifier's score	N1	183	42	41	41
	N2	26	1118	34	33
	SWS	23	83	742	17
	REM	86	35	34	489
Sensitivity		57.55%	87.48%	86.91%	84.31%
Accuracy		83.55%			
Kappa		0.76			

The main objective of this study is considering effective connectivity in SWS and REM sleep stages. However, just to show the potential of effective connectivity as a feature set, multiclass classification of other sleep stages is done. The provided results in multiclass classification are compared to some other recent studies in Table 9. By comparing the results in Table 9 it can be seen that although the efficiency of this study is lower than some others, the result is in an acceptable range in comparison to other studies.

3.1. Conclusion

The GPDC method was used in this study to estimate the effective connectivity of the brain from EEG signals. The estimated effective connectivities that are extracted from 12-channel EEG signals recorded from eight

Table 8. Confusion matrix and result of classifying epochs into four stages for subject-based approach.

		Expert's score			
		N1	N2	SWS	REM
Classifier's score	N1	178.26± 17.33	40.56±8.7	42.02±4.21	39.98±3.14
	N2	28.11±2.8	1114.16±83.12	36.78±9.12	34.15±5.60
	SWS	25.12±3.54	84.16±10.10	731.15±40.12	19.87±13.2
	REM	88.87±13.12	37.16±16.78	45.84±9.49	471.12±48.64
Sensitivity		55.64%	87.31%	85.44%	83.37%
Accuracy		82.72%			
Kappa		0.75			

Table 9. Comparison of the results with some other studies in multiclass classification sleep staging.

Study	Year	Accuracy	Kappa
Berthomier et al, [35]	2007	71.2	0.61
Liang et al. [47]	2012	78.0	0.68
Hsu et al. [49]	2013	87.2	0.80
Bajaj & Pachori [50]	2013	92.9	0.90
Zhu et al. [51]	2014	88.9	0.83
Hassan & Bhuiyan [52]	2017	83.5	0.84
This study		83.5	0.76

healthy subjects were used to extract SWS and REM sleep stages. First, it has been shown that there are some effective connectivities and their variations between channels that significantly vary by changing sleep stages as SWS versus non-SWS and REM versus non-REM. On the other hand, the results showed that the magnitude of the GPDC measure of significance in REM and non-SWS is greater than in the non-REM and SWS sleep stages, respectively. Also, the variation of the GPDC measure of brain connectivity in presented channels in REM and non-SWS is less than in non-REM and SWS sleep stages. This magnitude and the variation of GPDC were used as a feature vector to train the SVM classifier. The results of evaluation showed an acceptable and in some cases higher performance for the proposed method than other studies.

In many studies, effective connectivity methods are used to investigate brain function and the relation of brain regions. However, in this study, as an engineering research, an effective connectivity method was used as a feature extraction method from EEG signals and the proposed results as shown in Figures 1 and 2 can be considered in future studies to investigate the relation of brain regions in different sleep stages and their significations. The proposed method to detect SWS and REM can be used in other future works and other studies that need to indicate SWS or REM stage starts to trigger any stimulation system.

References

[1] AASM. The AASM Manual for the Scoring of Sleep and Associated Events-Rules. Terminology and Technical Specifications. Chicago, IL, USA: American Academy of Sleep Medicine, 2007.

[2] Van Cauter E, Spiegel K, Tasali E, Leproult R. Metabolic consequences of sleep and sleep loss. Sleep Med 2008; 9: 23-28.

[3] Van Cauter E, Leproult R, Plat L. Age-related changes in slow wave sleep and REM sleep and relationship with growth hormone and cortisol levels in healthy men. J Am Med Assoc 2000; 84: 861-868.

[4] Majde JA, Krueger JM. Links between the innate immune system and sleep. J Allergy Clin Immunol 2005; 116: 1188-1198.

[5] Tasali E, Leproult R, Ehrmann DA, Van Cauter E. Slow-wave sleep and the risk of type 2 diabetes in humans. P Natl Acad Sci USA 2008; 105: 1044-1049.

[6] Diekelmann S, Born J. The memory function of sleep. Nat Rev Neurosci 2010; 11: 114-126.

[7] Kyung Lee E, Douglass AB. Sleep in psychiatric disorders: where are we now? Can J Psychiatry 2010; 55: 403-412.

[8] Fung MM, Peters K, Redline S, Ziegler MG, Ancoli-Israel S, Barrett-Connor E, Stone KL. Decreased slow wave sleep increases risk of developing hypertension in elderly men. Hypertension 2011; 58: 596-603.

[9] Park HJ,Oh JS, Jeong DU, Park KS. Automated sleep stage scoring using hybrid rule-and case-based reasoning. Comput Biomed Res 2000; 33: 330-349.

[10] Agarwal R, Gotman J. Computer-assisted sleep staging. IEEE T Biomed 2001; 48: 1412-1423.

[11] Caffarel J, Gibson GJ, Harrison JP, Griffiths CJ, Drinnan MJ. Comparison of manual sleep staging with automated neural network-based analysis in clinical practice. Med Biol Eng Comput 2006; 44: 105-110.

[12] Poree F, Kachenoura A, Gauvrit H, Morvan C, Carrault G, Senhadji L. Blind source separation for ambulatory sleep recording. IEEE T Inf Technol Biomed 2006; 10: 293-301.

[13] Tagluk ME, Sezgin N, Akin M. Estimation of sleep stages by an artificial neural network employing EEG, EMG and EOG. J Med Syst 2010; 34: 717-725.

[14] Liang SF, Kuo CE, Hu YH, Cheng YS. A rule-based automatic sleep staging method. J Neurosci Methods 2012; 205: 169-176.

[15] Pan ST, Kuo CE, Zeng JH, Liang SF. A transition-constrained discrete hidden Markov model for automatic sleep staging. Biomed Eng Online 2012; 11: 52.

[16] Diekelmann S, Wilhelm I, Born J. The whats and whens of sleep-dependent memory consolidation. Sleep Med Rev 2009; 13: 309-321.

[17] Bellesi M, Riedner BA, Garcia-Molina GN, Cirelli C, Tononi G. Enhancement of sleep slow waves: underlying mechanisms and practical consequences. Front Syst Neurosci 2014; 8: 208.

[18] Huber R, Ghilardi MF, Massimini M, Ferrarelli F, Riedner BA, Peterson MJ, Tononi G. Arm immobilization causes cortical plastic changes and locally decreases sleep slow wave activity. Nat Neurosci 2006; 9: 1169-1176.

[19] Ngo HV, Claussen JC, Born J, Molle M. Induction of slow oscillations by rhythmic acoustic stimulation. J Sleep Res 2013; 22: 22-31.

[20] Tononi G, Riedner BA, Hulse BK, Ferrarelli F, Sarasso S. Enhancing sleep slow waves with natural stimuli. Medicamundi 2010; 54: 82-88.

[21] Ngo HV, Miedema A, Faude I, Martinetz T, Molle M, Born J. Driving sleep slow oscillations by auditory closed-loop stimulation–a self-limiting process. J Neurosci 2015; 35: 6630-6638.

[22] van Poppel EAM. Predicting brainwaves: The influence of auditory closed-loop cueing during slow oscillation up-states on vocabulary memory. MSc, University of Amsterdam, Amsterdam, the Netherlands, 2016.

[23] Papalambros NA, Santostasi G, Malkani RG, Braun R, Weintraub S, Paller KA, Zee PC. Acoustic enhancement of sleep slow oscillations and concomitant memory improvement in older adults. Front Hum Neurosci 2017; 11: 1-14.

[24] Ong JL, Lo JC, Chee NI, Santostasi G, Paller KA, Zee PC, Chee MW. Effects of phase-locked acoustic stimulation during a nap on EEG spectra and declarative memory consolidation. Sleep Med 2016; 20: 88-97.

[25] Leminen MN, Virkkala J, Saure E, Paajanen T, Zee PC, Santostasi G, Hublin C, Muller K, Porkka-Heiskanen T, Huotilainen M et al. Enhanced memory consolidation via automatic sound stimulation during non-REM sleep. Sleep 2017; 40: zsx00.

[26] Schabus M, Dang-Vu T, Heib D, Boly M, Desseilles M, Vandewalle G, Schmidt C, Albouy G, Darsaud A, Gais S et al. The fate of incoming stimuli during NREM sleep is determined by spindles and the phase of the slow oscillation. Front Neurol 2012; 3: 40.

[27] Lustenberger C, Boyle MR, Alagapan S, Mellin JM, Vaughn BV, Frohlich F. Feedback-controlled transcranial alternating current stimulation reveals a functional role of sleep spindles in motor memory consolidation. Curr Biol 2016; 26: 2127-2136.

[28] Kim YK, Park E, Lee A, Im CH, Kim YH. Changes in network connectivity during motor imagery and execution. PLoS One 2018; 13: e0190715.

[29] Parker CS, Clayden JD, Cardoso MJ, Rodionov R, Duncan JS, Scott C, Diehl B, Ourselin S. Structural and effective connectivity in focal epilepsy. Neuroimage Clin 2018; 17: 943-952.

[30] Jobst BM, Hindriks R, Laufs H, Tagliazucchi E, Hahn G, Ponce-Alvarez A, Stevner ABA, Kringelbach ML, Deco G. Increased stability and breakdown of brain effective connectivity during slow-wave sleep: mechanistic insights from whole-brain computational modelling. Sci Rep-UK 2017; 7: 4634.

[31] Geweke J. Measurement of linear dependence and feedback between multiple time series. J Am Stat Assoc 1982; 77: 304-324.

[32] Kaminski M, Blinowska KJ. A new method of the description of the information flow in brain structures. Biol Cybern 1991; 65: 203-210.

[33] Baccala LA, Sameshima K. Partial directed coherence: a new conception in neural structure determination. Biol Cybern 2001; 84: 463-474.

[34] Baccala LA, Sameshima K, Takahashi DY. Generalized partial directed coherence. In: IEEE 2007 15th International Conference on Digital Signal Processing. New York, NY, USA: IEEE. pp. 163-166.

[35] Berthomier C, Drouot X, Herman-Stoica M, Berthomier P, Prado J, Bokar-Thire D, Benoit O, Mattout J, D'Ortho MP. Automatic analysis of single-channel sleep EEGg: validation in healthy individuals. Sleep 2007; 30: 1587-1595.

[36] Seifpour S, Niknazar H, Mikaeili M, Nasrabadi AM. A new automatic sleep staging system based on statistical behavior of local extrema using single channel EEG signal. Expert Syst Appl 2018; 104: 277-293.

[37] Akaike H. Information theory and an extension of the maximum likelihood principle. In: 2nd International Symposium on Information Theory; 2–8 September 1971; Tsahkadsor, Armenia. Budapest, Hungary: Akademiai Kiad. pp. 267-281.

[38] Delorme A, Mullen T, Kothe C, Acar ZA, Bigdely-Shamlo N, Vankov A, Makeig S. EEGLAB, SIFT, NFT, BCILAB, and ERICA: New tools for advanced EEG processing. Comput Intell Neurosci 2011; 2011: 130714.

[39] Dietterich TG, Bakiri G. Solving multiclass learning problems via error-correcting output codes. arXiv 1994: Cs/9501101.

[40] Cohen JA. Coefficient of agreement for nominal scales. Educ Psyhol Meas 1960; 20: 37-46.

[41] Kreyszig E. Advanced Engineering Mathematics. 4th ed. New York, NY, USA: Wiley, 1979.

[42] Kubicki S, Holler L, Berg I, Pastelak-Price C, Dorow R. Sleep EEG evaluation: a comparison of results obtained by visual scoring and automatic analysis with the Oxford sleep stager. Sleep 1989; 12: 140-149.

[43] Durka PJ, Malinowska U, Szelenberger W, Wakarow A, Blinowska KJ. High resolution parametric description of slow wave sleep. J Neurosci Meth 2005; 147: 15-21.

[44] Virkkala J, Hasan J, Varri A, Himanen S, Muller K. Automatic detection of slow wave sleep using two channel electro-oculography. J Neurosci Methods 2007; 160: 171-177.

[45] Su B, Luo Y, Hong C, Nagurka ML, Yen C. Detecting slow wave sleep using a single EEG signal channel. J Neurosci Methods 2015; 243: 47-52.

[46] Imtiaz SA, Rodriguez-Villegas E. A low computational cost algorithm for REM sleep detection using single channel EEG. Ann Biomed Eng 2014; 42: 2344-2359.

[47] Liang S, Kuo C, Hu Y, Pan Y, Wang Y. Automatic stage scoring of single-channel sleep EEG by using multiscale entropy and autoregressive models. IEEE T Instrum Meas 2012; 61: 1649-1657.

[48] Ronzhina M, Janousek O, Kolarova J, Novakova M, Honzik P, Provaznik I. Sleep scoring using artificial neural networks. Sleep Med Rev 2012; 16: 251-263.

[49] Hsu YL, Yang YT, Wang JS, Hsu CY. Automatic sleep stage recurrent neural classifier using energy features of EEG signals. Neurocomputing 2013; 104: 105-114.

[50] Bajaj V, Pachori RB. Automatic classification of sleep stages based on the time-frequency image of EEG signals. Comput Methods Programs Biomed 2013; 112: 320-328.

[51] Zhu G, Li Y, Wen P. Analysis and classification of sleep stages based on difference visibility graphs from a single-channel EEG signal. IEEE J Biomed Health Inform 2014; 18: 1813-1821.

[52] Hassan AR, Bhuiyan MI. Automated identification of sleep states from EEG signals by means of ensemble empirical mode decomposition and random under sampling boosting. Comput Methods Programs Biomed 2017; 140: 201-210.